Probabilistic failure assessment of oil pipelines due to internal corrosion

Khakzad, Sina; Yang, Ming; Lohi, Ali; Khakzad, Nima

DOI
10.1002/prs.12364

Publication date
2022

Document Version
Final published version

Published in
Process Safety Progress

Received: 8 January 2022 | Revised: 7 March 2022 | Accepted: 23 March 2022

DOI: 10.1002/prs.12364

PROCESS SAFETY PROGRESS

ORIGINAL ARTICLE

Probabilistic failure assessment of oil pipelines due to internal corrosion

Sina Khakzad[1] | Ming Yang[2] | Ali Lohi[3] | Nima Khakzad[4]

[1]Faculty of Engineering and Applied Science, Memorial University of Newfoundland, St. John's, Canada

[2]Faculty of Technology, Policy, and Management, Delft University of Technology, Delft, The Netherlands

[3]Department of Chemical Engineering, Ryerson University, Toronto, Canada

[4]School of Occupational and Public Health, Ryerson University, Toronto, Canada

Correspondence
Nima Khakzad, School of Occupational and Public Health, Ryerson University, 288 Church Street, Toronto, M5B 1Z5, Canada.
Email: nima.khakzad@ryerson.ca

Funding information
Publication Grant, Faculty of Community Services, Ryerson University

Abstract

Oil and gas pipelines play a key role in the safe and efficient delivery of energy resources around the world. Crude oil by itself is not corrosive, but oil extracted from geological reservoirs is accompanied by varying amounts of water and acidic gases such as carbon dioxide (CO_2), which can form a corrosive combination. Estimating the corrosion rate and depth in pipelines is essential for predicting their failure probability. In the present study, a Bayesian network has been developed for predicting the distribution of corrosion rate in oil pipelines given the point estimates generated using an empirical corrosion simulation model. For this purpose, the simulation model considers corrosion parameters such as pipe diameter, flow temperature, flow velocity, and CO_2 partial pressure, among others. With the corrosion rate distribution predicted by the Bayesian network, corrosion depth–rate relationships have been employed to convert the corrosion rate distribution into failure probability distribution.

KEYWORDS
Bayesian network, depth–rate relationship, failure probability assessment, oil pipeline

1 | INTRODUCTION

Pipelines are still considered the safest and most cost-effective means of mass transportation in the oil and gas industry. Meanwhile, even minor failures in pipelines may lead to catastrophic consequences.[1] Among the failure modes of pipelines, corrosion appears to be one of the most feared and frequent culprits. Corrosion is a naturally occurring electrochemical reaction resulting in the degradation of materials.

Corrosion of pipelines by aqueous CO_2 and H_2S has long been a concern in the oil and gas industry and still represents a serious threat to pipeline integrity and plays a key role in life-cycle assessment of oil pipelines.[2] Oil and gas pipelines are commonly made of carbon steel because of its good mechanical properties, low cost, and wider availability despite having a relatively low corrosion resistance.[3] Applying advanced techniques in oil and gas extraction, such as CO_2 injection for enhanced oil recovery and extraction of deep natural gas reservoirs, has brought this problem to attention again.[4]

Dry gas and oil by themselves are not corrosive; however, the presence of an aqueous phase on the metal surface along with CO_2 and H_2S provides a suitable condition for corrosion to occur.[5] When oil wells age, the production of oil starts to decline whereas the flow rates of water and gas, which usually contain corrosive agents such as CO_2, start to increase, accelerating the internal corrosion of the pipeline.[3,6]

Abbreviations: BN, Bayesian network; d, Corrosion depth; D, Pipe diameter; $f(r)$, Probability density function of corrosion rate; $F(R)$, Cumulative density function of corrosion rate; h, Pipe wall thickness; I, Inhibitor efficiency; k, Shape parameter of Weibull distribution; P, Pressure; pCO_2, Partial pressure of CO_2; POF, Probability of failure; r, Corrosion rate variable; R, Corrosion rate value; t, Age of pipe (exposure time to corrosion); S, Shear stress; T, Temperature; V, Flow velocity; X, Generic random variable in BN; α, Exponent of corrosion depth function; β, Coefficient of corrosion depth function; θ, Parameters (conditional probabilities) of BN; γ, Scale parameter of Weibull distribution.

Although there are steel alloys that resist corrosion effectively, mild steel (a type of carbon steel with low carbon content) is widely used in the construction of pipelines and process equipment in the oil and gas industry, because of its cost effectiveness. The corrosive environment in the presence of acidic gases of CO_2 and H_2S is classified as sweet and sour corrosion, respectively.[7] The severity of both types of corrosion is controlled by the combination of several operational parameters such as temperature, pressure, flow velocity, and the environmental parameters such as the pH of the fluid inside the pipeline.

Data about the rate and extent of corrosion are usually collected by intelligent pigging, which is a highly sophisticated instrument for measuring the pipeline wall thickness through electromagnetic waves or electrochemical potential noise.[8] If the corrosion rate cannot be determined from thickness inspection data, rough estimates may be established using expert elicitation,[9] or predictions can be made using deterministic and probabilistic models based on measurement of the key corrosion parameters.[10–18] Generic failure frequencies of process equipment and pipelines, due to internal and external corrosion, are also available[19] but they need to be tailored before use by taking factors such as management systems, inspection history, an so on, into account.

Based on the underlying physicochemical processes of corrosion, many models have been developed to calculate the corrosion rate of pipelines, including mechanistic models,[14,20] semiempirical models,[21] empirical models,[22,23] neural networks,[24,25] and numerical simulation of corrosion differential equations.[26] The Bayesian network (BN) has been effectively used for modeling and failure assessment of engineering systems and structures where uncertainty may impede the application of conventional techniques.[27] BNs developed or enhanced on the basis of physical models (also known as physical-model-based BNs) have recently been employed as a promising alternative for corrosion analysis[28–32] and for estimating the remaining useful life and reliability of pipelines[33] and for other engineering systems.[34,35] The superior performance of BN over most conventional techniques is mainly due to its ability in reasoning under uncertainty and updating the prior probabilities should new information become available.

In the present study, a probabilistic method based on BN and Weibull distribution is proposed for predicting the failure probability of an oil pipeline due to CO_2 corrosion. Considering the radial corrosion rate as a key factor in corrosion-related failure of pipelines,[14] a corrosion rate simulation model[23] is used to generate point estimates of corrosion rate (mm/year) given the pipe diameter, flow temperature, flow velocity, CO_2 concentration (as its partial pressure), and so on. The output of the simulation model is used to develop a BN and learn its parameters via the maximum likelihood estimation algorithm. With the distribution of the corrosion rate predicted by the BN, a Weibull distribution is used to predict the corrosion depth and the respective failure probabilities.

The steps taken to develop the methodology are illustrated in Figure 1.

In Section 2, the basics of CO_2 corrosion and BN are briefly reviewed (Step 1 is covered in Section 2.1). Section 3 demonstrates the development and validation of the developed BN model for predicting corrosion rates through an illustrative case study (Step 2 is covered in Section 3.1 while Step 3 is covered in Section 3.2). In Section 4, a Weibull distribution is used to estimate the corrosion depth and predict the respective failure probabilities (Step 4 is covered in Section 4). Section 5 concludes the paper.

2 | THEORETICAL BACKGROUND

2.1 | CO_2 corrosion mechanism

The initiation of corrosion damage is a random process, depending on the microstructure of the material, the surface condition (e.g., the

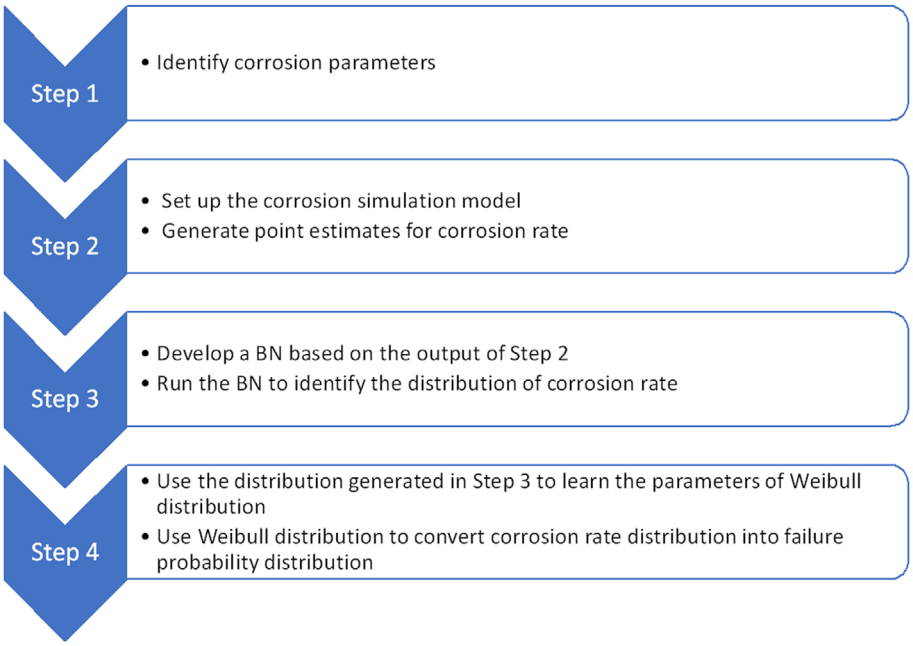

FIGURE 1 Steps taken to generate the failure probability distribution in the present study

presence of surface defects), and other environmental factors.[17] Aqueous CO_2 corrosion of mild steel is an electrochemical process involving the anodic dissolution of iron (Fe) and the cathodic evolution of hydrogen (H_2) as[3]

$$Fe + CO_2 + H_2O \rightarrow FeCO_3 + H_2. \quad (1)$$

The presence of CO_2 can increase the rate of hydrogen evolution and thus accelerate the rate of corrosion. As an oil well ages, the production of oil starts to decline, whereas the flow of water and gas, which usually contain highly corrosive agents such as CO_2, tends to increase. This, in turn, accelerates the corrosion process inside the pipeline.[3] Compared to that of CO_2, the role of iron carbonate ($FeCO_3$), which is usually formed at higher temperatures in the form of solid films (also known as scales), is twofold: it can be protective and decelerate the corrosion, or it could be non-protective, depending on the environmental conditions under which it is created.[36] Iron can also be anodically dissolved individually in acid solutions as

$$Fe \rightarrow Fe^{2+} + 2e^-. \quad (2)$$

As a result, carbonic acid (H_2CO_3) can react with free electrons and enable hydrogen evolution even at pH >5:

$$2H_2CO_3 + 2e^- \rightarrow H_2 + 2HCO_3^-. \quad (3)$$

However, carbonic acid is believed to serve as an extra source of hydrogen ions (H^+), which in retraction with electrons can lead to the evolution of more hydrogen:

$$2H^+ + 2e^- \rightarrow H_2. \quad (4)$$

pH has a strong influence on corrosion rate; at pH ≤4, the reduction of H^+ ions is important particularly at lower partial pressures of CO_2 (pCO_2), directly affecting the corrosion rate. On the other hand, at high pH the solubility of iron carbonate decreases, which in turn increases the precipitation rate and formation of scales, thereby reducing the rate of corrosion.[7]

pCO_2, temperature, flow velocity, and corrosion inhibitor are the other factors that play a key role in the rate of corrosion.[36] The increase in pCO_2 increases the concentration of carbonic acid and accelerates the cathodic reaction and thus the corrosion rate. The role of temperature, however, is controversial: at low pH, the increase in temperature accelerates the corrosion rate, whereas at high pH, a high temperature speeds up the formation of protective scales and decreases the corrosion rate. By almost all accounts, flow velocity at both low and high pH increases the rate of corrosion. Given the corrosion depth (d) and the pipe wall thickness (h), the corrosion depth can be categorized as shallow if $0.1 < \frac{d}{h} < 0.2$, moderately deep if $0.2 < \frac{d}{h} < 0.4$, and deep if $0.4 < \frac{d}{h} < 0.6$.[15] A detailed analysis of CO_2 corrosion mechanism can be found elsewhere.[3]

2.2 | Bayesian network

A BN can be defined as an acyclic directed graph $BN = (G, \theta)$, where G denotes the structure of the graph (nodes and edges) and θ denotes the parameters.[37] Based on the chain rule and the d-separation criteria, the joint probability distribution of the nodes (each node represents a random variable) in a BN can be factorized as the product of the conditional probabilities of the nodes given their immediate parents

$$P(X_1, X_2, ..., X_n) = \prod_{i=1}^{n} P(X_i | pa(X_i)), \quad (5)$$

where X_i is a random variable, and $pa(X_i)$ is the parent set of X_i, that is, the set of nodes from which there are direct edges to X_i. The conditional probabilities $\theta_i = P(X_i|pa(X_i))$, which are also known as the parameters, can either be estimated by subject matter experts or be learned from data (observations) using algorithms such as the maximum likelihood estimation (MLE).

Given a set of observations $D = \{d_1, d_2, ..., d_m\}$ in which each observation assigns a value to each node as $d_j = \left\{x_1^j, x_2^j, ..., x_n^j\right\}$, the likelihood function of the parameters can be developed as[38]

$$L(D; G, \theta) = P(D|\theta) = \prod_{j=1}^{m} P(d_j|\theta) = \prod_{j=1}^{m} \prod_{i=1}^{n} P\left(x_i^j | pa\left(x_i^j\right)\right). \quad (6)$$

By maximizing either the likelihood function in Equation (6) or its natural logarithm (log-likelihood function), the parameters of the BN can be estimated. An illustrative example on the application of MLE is presented in the Appendix A.

3 | MODEL DEVELOPMENT

3.1 | Data generation

Considering the influential parameters in CO_2 corrosion, as described in Section 2.1, the M-506 corrosion rate model, which is an empirical model developed by NORSOK,[23] is used to generate the data required for estimating the conditional probabilities of the BN model for predicting the corrosion rates. If experimental data or field measurements are available,[39] the probabilities needed in the BN can be estimated using data mining techniques. In the present study, for illustrative purposes, the data generated by the M-506 model is used for model development and parameter learning.

The M-506 has been developed using Microsoft Excel and has a main dialogue box (Figure 2) that can perform all corrosion rate calculations with no need for (or the possibility of) changing the program settings. All the input parameters can be entered in the dialogue box for point calculation of the corrosion rate (mm/year). The model is based on the NORSOK Standard M-506 and is developed by the

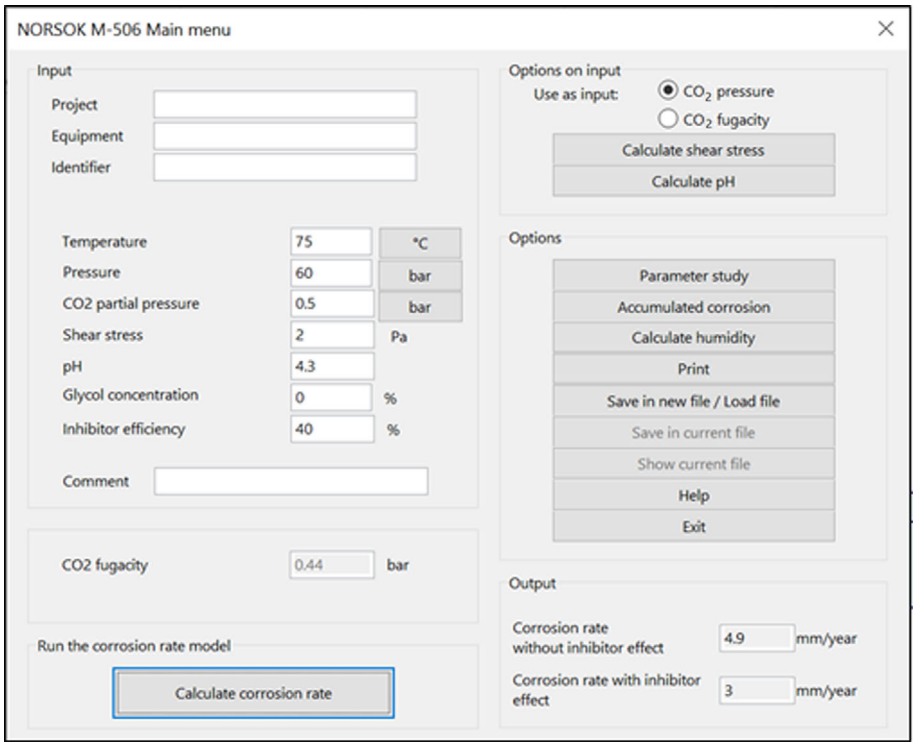

FIGURE 2 Interface of M-506 corrosion rate model[23]

Temperature (*T*)	Pressure (*P*)	pCO_2	Flow velocity (*V*)	pH
60–75°C	60–70 bar	0.3–0.5 bar	0.7–1.6 m/s	3.5–5.5

TABLE 1 Experimental values of corrosion parameters[36] used in the M-506 model[23] for data generation

Norwegian Oil Industry Association and the Federation of Norwegian Manufacturing Industries.[40]

The M-506 uses, among other parameters, the flow temperature and pressure, flow velocity, and the internal diameter of the pipe to calculate the shear stress on the internal wall of the pipe. Similarly, the temperature, pressure, and pCO_2 are used to calculate the pH. Having the shear stress, pH, and efficiency of corrosion inhibitor, the M-506 calculates a single value for the corrosion rate (mm/year). The steps taken to enter the input parameters in the M-506 simulator are as follow:

- Step 1. Insert the fluid temperature (in °C) in the Temperature box.
- Step 2. Insert the internal pressure (in bar) in the Pressure box.
- Step 3. Insert the CO_2 partial pressure (in bar) in the box with the same name.
- Step 4. Click "Calculate shear stress" to calculate the shear stress. The calculated value will automatically appear in the Shear stress box (in Pa).
- Step 5. Click "Calculate pH" to calculate the fluid pH. The calculated value will automatically appear in the pH box.
- Step 6. If glycol has been added to the fluid to prevent it from freezing, insert its concentration in the Glycol concentration box (in %).
- Step 7. Insert the efficiency of the corrosion inhibitor in the Inhibitor efficiency box (in %).
- Step 8. Press the "Calculate corrosion rate" button to run the model and calculate the corrosion rate (in mm/year). The model calculates the corrosion rate both in the presence and absence of the corrosion inhibitor.

The model is valid for temperatures 5–150°C, pH 3.5–6.5, shear stress 1–150 Pa, and pCO_2 0.1–10 bar, although it may mis-predict the corrosion rate when pCO_2 is less than 0.5 bar. The model is applicable to corrosion rates only when CO_2 is the corrosive agent. In other words, it does not include the additional effects of other constituents that may influence the corrosivity, including contamination of O_2 and H_2S, which are more common in water and gas pipelines.

To validate the developed BN in Section 3.2, the experimental values reported in Peng and Zeng[36] for the temperature (*T*), pCO_2, and flow velocity (*V*) are adopted in the present study, as listed in Table 1.

As the same parameters will be used for the root nodes of the BN, to facilitate the discretization of the nodes later in Section 3.2, the values reported in Table 1 were discretized as $T = (60, 70, 75)$, $P = (60, 65, 70)$, $pCO_2 = (0.3, 0.4, 0.5)$, and $V = (0.7, 1.1, 1.6)$. Further, since the inhibitor efficiency is not reported in Peng and Zeng,[36] three values were considered for the inhibitor efficiency (%) as $I = (40, 50, 60)$. Owing to the uncertainty regarding the distributions of the basic parameters (the root nodes), uniform distribution was considered for all the root nodes so as to not impose the analyst's prior (and possibly biased) knowledge on the analysis; this way, given a root node, all the states of the node would have equal chances to contribute to the probability distribution of the corrosion rate and consequently the failure probability. Considering a wall thickness of 12 mm for the pipeline of interest, the M-506 model was run 243 times to account for all

TABLE 2 Sample of data generated using the M-506 model[23]

T (°C)	P (bar)	pCO_2 (bar)	V (m/s)	I (%)	pH	Shear (Pa)	Corrosion rate (mm/year)
60	60	0.5	1.1	40	4.2	2	3.2
70	65	0.3	0.7	50	4.4	1	1.6
60	70	0.5	1.6	50	4.2	4	2.7
75	70	0.4	1.6	40	4.3	4	2.8

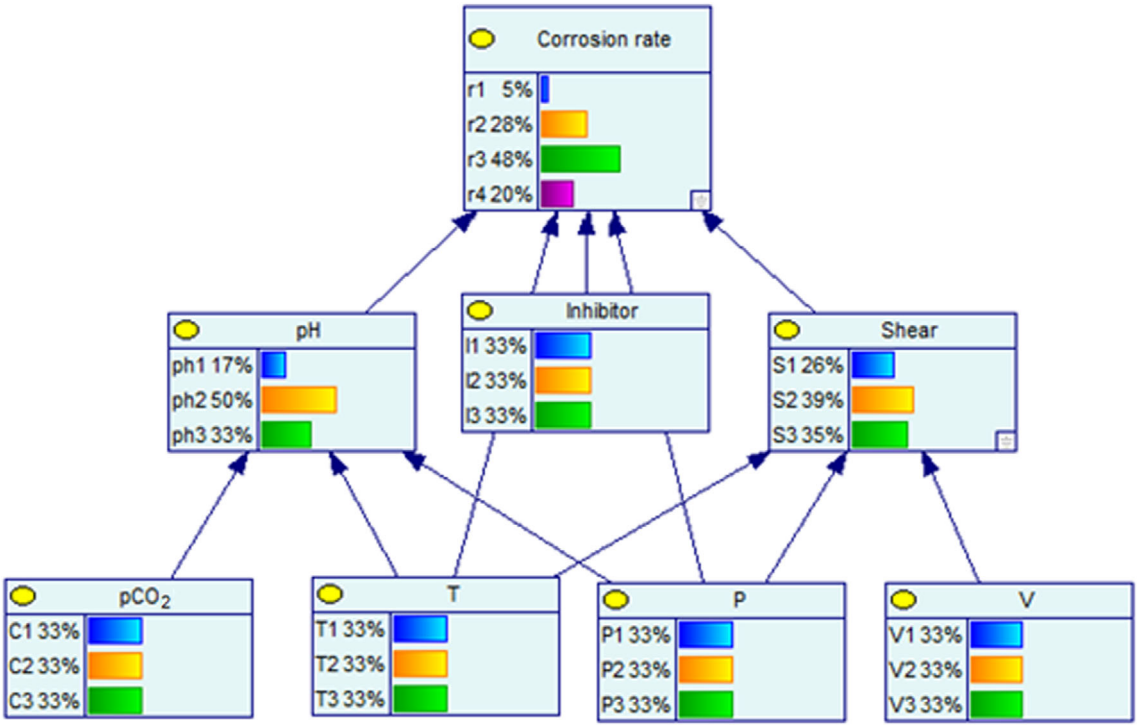

FIGURE 3 BN developed for predicting CO_2 corrosion rate

possible combinations of the five tertiary root nodes ($3^5 = 243$). Given the input parameters, the discrete values of pH and shear stress were calculated by the model as pH = (4.2, 4.3, 4.4) and Shear = (1, 2, 4) while the corrosion rates were observed to vary from 1 to 4 mm/year. A sample of the generated data is presented in Table 2.

3.2 | Development of the Bayesian network

The parameters and the way they are considered by the M-506 to calculate the shear stress, pH, and, finally, the corrosion rate can be used to construct the structure (nodes and the causal arcs, among others) of the BN, as shown in Figure 3. Since the M-506 uses the temperature, pressure, and flow velocity to calculate the shear stress, the corresponding nodes are considered as the parents of the node Shear (shear stress) in the BN. Similarly, since the M-506 uses the temperature, pressure, and pCO_2 to calculate the pH, the corresponding nodes are considered as the parents of the node pH in the BN. The nodes T, P, pH, and Shear, together with the node Inhibitor (inhibitor efficiency), are connected to the node Corrosion rate as its parents. The nodes of the BN and their states are presented in Table 3.

Using data generated in Section 3.1, the parameter learning module of the GeNIe software[41] was employed to learn the conditional probabilities of the nodes pH, Shear, and Corrosion rate in the BN using the MLE algorithm presented in Equation (6). Since the values of corrosion rate were continuous and varying from 1 to 4 mm/year, for the corresponding node in the BN, four discrete states were considered as $r1$ = 0–1 mm/year, $r2$ = 1–2 mm/year, $r3$ = 2–3 mm/year, and $r4$ = 3–4 mm/year.

With the parameter learning implemented, the BN was quantified to obtain the probability distribution of the corrosion rates as $P(r1, r2, r3, r4)$ = (0.05, 0.28, 0.48, 0.20), with the corrosion rate of 2–3 mm/year as the likeliest corrosion rate with a probability of ∼48%. This is in agreement with the experimental result reported in Peng and Zeng,[36] where an average corrosion rate of ∼3–4 mm/year was reported. The reason why the experimentally measured corrosion rate is slightly higher than the one predicted by the BN can be explained as due to a more acidic condition (pH = 3.5–4) in the experiments conducted by Peng and Zeng,[36] which could not be exactly simulated using the M-506 model. This is because the M-506 calculates pH as a function of T, P, and pCO2, without letting the analyst to arbitrarily set or manipulate its value.

TABLE 3 The nodes of the BN in Figure 3 and their states. The probability distributions of the root nodes are identified by the user (uniform distribution), while the distributions of the child nodes are identified by the BN using the maximum likelihood function

Parameter	Node	States	Probability distribution
Temperature (°C)	*T*	*T*1 = 60 *T*2 = 70 *T*3 = 75	(0.33, 0.33, 0.33)
Pressure (bar)	*P*	*P*1 = 60 *P*2 = 65 *P*3 = 70	(0.33, 0.33, 0.33)
CO_2 pressure (bar)	pCO2	*C*1 = 0.3 *C*2 = 0.4 C3 = 0.5	(0.33, 0.33, 0.33)
Flow velocity (m/s)	*V*	*V*1 = 0.7 *V*2 = 1.1 *V*3 = 1.6	(0.33, 0.33, 0.33)
Inhibitor efficiency (%)	Inhibitor	*I*1 = 40 *I*2 = 50 *I*3 = 60	(0.33, 0.33, 0.33)
pH	pH	pH 1 = 4.2 pH 2 = 4.3 pH 3 = 4.4	(0.17, 0.50, 0.33)
Shear stress (Pa)	Shear	*S*1 = 1 *S*2 = 2 *S*3 = 4	(0.26, 0.39, 0.35)
Corrosion rate (mm/year)	Corrosion rate	*r*1 = 0–1 *r*2 = 1–2 *r*3 = 2–3 *r*4 = 3–4	(0.05, 0.28, 0.48, 0.20)

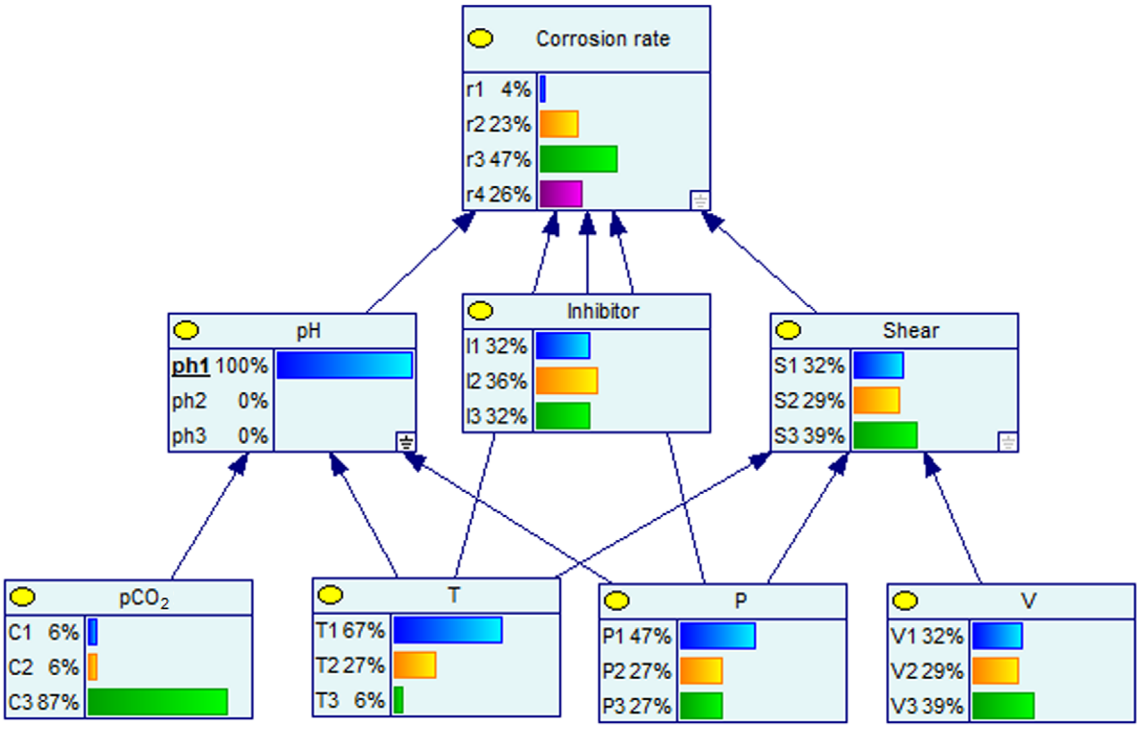

FIGURE 4 Updated BN given an instantiation of pH node. Corrosion rate distribution is skewed to the right, given a more acidic pH

To examine the impact of pH on the corrosion rate, node pH was instantiated to pH 1 = 4.2, which is the most acidic state among the others, to update the states of node Corrosion rate. As can be noted from the updated BN in Figure 4, this more acidic pH makes the probability distribution of Corrosion rate more skewed to the right, increasing the probability of *r*4 = 3–4 mm/year from 0.2 (in Figure 3)

and 0.26 (in Figure 4). As such, a more acidic pH (3.5–4) would be expected to further increase the likelihood of $r = 3$–4 mm/year in the BN, making the prediction even more consistent with the experiment.

4 | ESTIMATION OF FAILURE PROBABILITY

The aim of pipeline corrosion analysis is to estimate the residual strength and failure probability of pipelines with the purpose of risk assessment or identifying maintenance schedules. One approach to relate the corrosion rate to the probability of failure (POF) of the pipeline is to first find the corrosion depth given the age of the pipe, and then to calculate the failure pressure of the corroded pipeline. Based on a comparison between the failure pressure of the corroded pipeline and the operational pressure of the pipeline,[14,15,18,42] the POF of the pipeline can be estimated using, among others, Monte Carlo simulation. This approach, however, is computationally demanding since both the corrosion width and length need to be calculated in addition to the corrosion depth.

One simpler approach is based on a comparison between the corrosion depth and the nominal wall thickness of the pipe.[9] As pointed out in Larin et al.,[17] at the operational pressure, a corroded pipe may incur plastic strains at spots where the corrosion depth (d) is larger than half of the pipe thickness (h). They also argue that at startup and shutdown pressures, which may be twice the operational pressure of the pipe, there is a 70% probability of failure where the corrosion depth is about one-third of the pipe thickness.

Following the latter approach (i.e., a comparison between the corrosion depth and the nominal wall thickness), in the present study we assume that the POF of the pipeline is conservatively equal to the probability of the corrosion depth exceeding one-third of the pipe wall thickness, that is

$$POF = P(d \geq 0.3h). \tag{7}$$

This assumption is also in agreement with that in Opeyemi et al.,[43] where the failure probabilities were obtained for $\frac{d}{h} \geq 0.3$, and in Hasan et al.,[44] where $0.15 < \frac{d}{h} < 0.40$ was proposed.

Therefore, if the corrosion depth and its distribution can be predicted based on the calculated corrosion rates, Equation (7) can be employed to derive the failure probability distribution of the corroded pipeline. In the next sections, we present two approaches to do so. In the first approach (Section 4.1), the corrosion rate predicted by the BN is assumed to have a Weibull distribution,[16,45] whereas in the second approach (Section 4.2) the corrosion rate predicted by the BN is directly employed with no further assumption regarding its distribution.

4.1 | First approach

Velazquez et al.[46] proposed that the growth of corrosion depth in low-carbon steel is a power-law function of the corrosion rate and the age (exposure time) of the pipeline:

$$d = r.t^{\alpha}, \tag{8}$$

where r is the corrosion rate, and α is the exponential factor identified based on experimental data, ranging from 0.3 to 1.0; Larin et al.[17] proposed the value of $\alpha = 0.6$. Similar power-law functions have been proposed for uniform internal corrosion of pipelines.[47-49] Considering the relationship between time, corrosion rate, and corrosion depth in Equation (8), the POF modeled in Equation (7) can be presented as

$$POF = P(d \geq 0.3h) = P(r.t^{0.6} > 0.3h) = P\left(r > \frac{0.3h}{t^{0.6}}\right). \tag{9}$$

Using the probability distribution of the corrosion rate, the POF presented in Equation (9) can be calculated. Corrosion rate, as a random variable, is commonly believed to satisfy the Gamma, Weibull, or generalized extreme value distributions.[16,45] In the present study, we adopt a Weibull distribution for the corrosion rate, with a probability density function $f(r)$ and cumulative density function $F(R)$ as

$$f(r) = \frac{k}{\gamma}\left(\frac{r}{\gamma}\right)^{k-1} e^{-\left(\frac{r}{\gamma}\right)^{k}}, \tag{10}$$

$$F(R) = P(r \leq R) = 1 - e^{-\left(\frac{R}{\gamma}\right)^{k}}, \tag{11}$$

where $k > 0$ and $\gamma > 0$ are, respectively, the shape parameter and the scale parameter of Weibull distribution. Considering temporal variation of corrosion rate, a value of $k < 1$ indicates a decreasing corrosion rate, $k = 1$ indicates a constant corrosion rate, and $k > 1$ indicates an increasing corrosion rate over time. By combining Equations (9) and (11), the POF can be calculated using Equation (12) if the values of k and γ are known:

$$POF = P\left(r > \frac{0.3h}{t^{0.6}}\right) = 1 - P\left(r < \frac{0.3h}{t^{0.6}}\right) = e^{-\left(\frac{0.3h}{\gamma t^{0.6}}\right)^{k}}. \tag{12}$$

The probability distribution of the corrosion rates predicted by the BN in Figure 3 can be used to estimate the values of k and γ for Equation (12). Since there are two unknown variables (k and γ), two equations would be required. Considering the corrosion rate probabilities, one equation can be $P(2 \leq r < 3) = 0.478$ while the other can be $P(3 \leq r < 4) = 0.196$ (any other two interval probabilities could be used for this purpose). Considering a nominal wall thickness of $h = 12$ mm for the pipeline, the foregoing equations would result in

$$\begin{cases} P(2 \leq r < 3) = 0.478 \\ P(3 \leq r < 4) = 0.196 \end{cases} \overset{\text{using (11)}}{\Rightarrow} \begin{cases} e^{-\left(\frac{2}{\gamma}\right)^{k}} - e^{-\left(\frac{3}{\gamma}\right)^{k}} = 0.478 \\ e^{-\left(\frac{3}{\gamma}\right)^{k}} - e^{-\left(\frac{4}{\gamma}\right)^{k}} = 0.196 \end{cases}. \tag{13}$$

Solving the system of equations presented in Equation (13) using Solver (a Microsoft Excel add-in program), the values of k and γ were obtained as 3.5 and 2.6, respectively. With $h = 12$ mm, the values of $k = 3.5$ and $\gamma = 2.6$, the cumulative POFs of the pipeline presented in Equation (12) can be updated as

$$POF(t) = e^{-\left(\frac{0.3h}{\gamma t^{0.6}}\right)^{k}} = e^{-\left(\frac{0.3\times 12}{2.6 t^{0.6}}\right)^{3.5}} = e^{-(3.12 t^{-2.1})}. \quad (14)$$

Using Equation (14), the failure probability distribution of the pipeline can be presented, as in Figure 6. For example, at $t = 3$ years, the cumulative failure probability is calculated as $POF(3) = e^{-(3.12\times 3^{-2.1})} = 0.73$.

4.2 | Second approach

The corrosion depth in uniform corrosion mechanisms can be modeled as a power-law function of the exposure time as[47-49]

$$d = \beta . t^{\alpha}, \quad (15)$$

where d is corrosion depth, t is exposure time, and α and β are constants to be determined using experimental or field measurements of d. Assuming a constant (but random) corrosion rate over time, β would be equal to r, and α would be equal to 1.0. Thus, Equation (15) can be simplified as

$$d = r.t. \quad (16)$$

Plugging Equation (16) in Equation (7), the failure probability can be calculated as

$$POF = P(d \geq 0.3h) = P(r.t \geq 0.3h) = P\left(r \geq \frac{0.3h}{t}\right). \quad (17)$$

With $h = 12$ mm, the probability mass distribution derived from the BN for the corrosion rate can be used to quantify Equation (17) for different values of t. This mass distribution is presented in Figure 5 for clarity. For instance, for $t = 1$ year, Equation (17) would be quantified as

$$POF(t=1) = P\left(r \geq \frac{0.3\times 12}{1}\right) = P(r \geq 3.6) = 1 - P(r < 3.6)$$
$$= 1 - \{P(0 \leq r < 1) + P(1 \leq r < 2) + P(2 \leq r < 3) + P(3 \leq r < 3.6)\}. \quad (18)$$

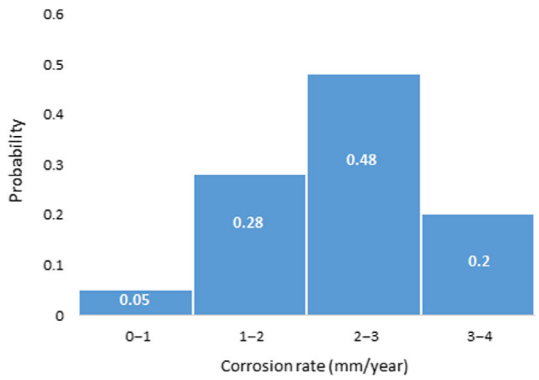

FIGURE 5 Corrosion rate mass distribution derived from BN in Figure 3

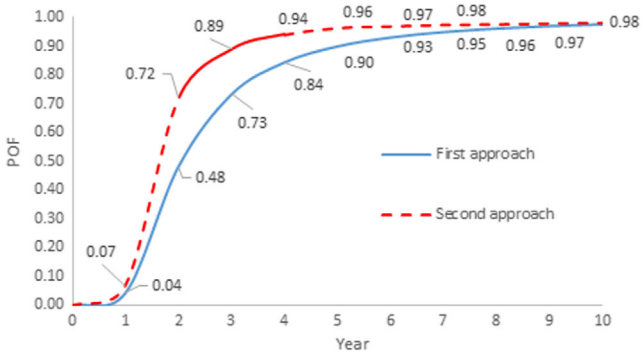

FIGURE 6 Failure probability distributions. The Second approach has resulted in higher failure probabilities due to the assumption of constant corrosion rate over time

According to Figure 5, $P(0 \leq r < 1) = 0.05$, $P(1 \leq r < 2) = 0.28$, and $P(2 \leq r < 3) = 0.48$. Further, assuming that the probability mass is equally spread over the corrosion interval $r = [3, 4)$, $P(3 \leq r < 3.6) = 0.6 \times 0.20 = 0.12$. Having the constituent probabilities, POF $(t = 1) = 1 - (0.05 + 0.28 + 0.48 + 0.12) = 0.07$.

The probability of failures for other consecutive years can be calculated similarly. The resultant probability distribution (second approach) is depicted in Figure 6 along with the results obtained from the first approach. The area with meaningful differences between the results is denoted with a red solid line, where the failure probabilities calculated by the second approach are higher than those of the first approach for $t = 2$, 3 and 4 years.

The higher failure probabilities in the second approach can be attributed to higher corrosion depths calculated using Equation (16) than Equation (8). This becomes clearer when we note that Equation (16) is a special case of Equation (8) in which $\alpha = 1.0$. In Equation (8), the role of α (0.3–1.0) is to consider the decelerating effect of environmental and corrosion parameters (e.g., corrosion scale) on the corrosion rate as time passes.

Corrosion scales consist of hard mineral coatings, and corrosion deposits build up over time at the location of corrosion, providing a protection layer and reducing the corrosion rate.[50] Since most empirical models assume constant corrosion rates, deceleration of the corrosion rate can be taken into account through the value of α. In other words, $\alpha < 1$ denotes a corrosion depth advancing with a decreasing pace (slowing corrosion rate), whereas $\alpha = 1$ denotes a corrosion depth increasing with a constant rate (constant corrosion rate). Therefore, the difference between the failure probabilities can partly be attributed to the assumption of a more aggressive corrosion rate in the second approach ($\alpha = 1.0$) than the first approach ($\alpha = 0.6$).

5 | CONCLUSIONS

In this study, we presented a methodology based on BN for predicting the probability distribution of corrosion rate in oil pipelines. An empirical model, namely the M-506 corrosion rate

simulator,[23] was used to generate the data required for the development and parameter learning of the BN. The corrosion rate probability distribution predicted by the BN was shown to be consistent with the experimental results.[36] Compared with the empirical model, the BN model was shown to account for the uncertainty of input variables, enabling the analyst to easily update the probability distribution of corrosion rate when new information (e.g., new data for oil temperature and pressure) becomes available. This updating feature of the BN is particularly important because recalibration of parameters in semiempirical and empirical models based on new data can usually be a tedious task.[24]

We demonstrated that the result of the BN (i.e., probability distribution for the corrosion rate) can be combined with corrosion depth–rate relationships to convert the corrosion rate's probability distribution into the pipeline's failure probability distribution. To do so, the rate distribution was processed under two separate assumptions, resulting in two approaches: In the first approach, the rate distribution was considered to have a Weibull distribution and a power-law function for the corrosion depth–rate relationship was used to imply that the corrosion rate might decelerate over time. In the second approach, however, the rate distribution derived from the BN was used with no further assumption regarding its distribution type, and a linear corrosion depth–rate relationship was employed to denote that the corrosion rate remains constant over time. Both approaches were illustrated to result in similar trends for the failure probability distribution, although, overall, the linear depth–rate relationship yields higher failure probabilities.

With new information regarding the input parameters, the developed methodology can be used to update the distributions of both the corrosion rate and the failure probability. To do so, the BN can be used directly to update the rate distribution, which can subsequently be used to update the failure distribution. For instance, regarding the first approach (Section 4.1), given an updated rate distribution, Equation (13) can be re-solved to calculate the updated values of k and γ (the parameters of Weibull distribution), and then Equation (14) can be recalculated using these updated k and γ to obtain updated failure probabilities.

The present study has not been aimed at advertising or validating the M-506 model; but it was to demonstrate how empirical models like M-506 can be coupled with BN and corrosion depth–rate relationships to predict the corrosion-induced failure of pipelines. As such, the accuracy of the method is expected to improve if more accurate models than the M-506 were employed.

ACKNOWLEDGMENTS

The authors are grateful to the two reviewers for their instructive comments that helped enhance the readability and quality of this study. The financial support provided by the Faculty of Community Services, Ryerson University, via the Publication Grant is much appreciated.

CONFLICT OF INTEREST

The authors declare no conflict of interest.

AUTHOR CONTRIBUTIONS

Sina Khakzad: Formal analysis (lead); methodology (lead); writing – original draft (lead). **Ming Yang:** Validation (equal); writing – review and editing (equal). **Ali Lohi:** Validation (equal); writing – review and editing (equal). **Nima Khakzad:** Conceptualization (lead); supervision (lead); writing – review and editing (lead).

DATA AVAILABILITY STATEMENT

The data that support the findings of this study are available from the corresponding author, [NK], upon reasonable request.

ORCID

Nima Khakzad https://orcid.org/0000-0002-3899-6830

REFERENCES

1. Khakzad S, Khan F, Abbassi R, Khakzad N. Accident risk-based life cycle assessment methodology for green and safe fuel selection. *Proc Safety Environ Protect*. 2017;109:268-287.
2. Bonis MR, Crolet JL. *Basics of the Prediction of the Risks of 2 CO Corrosion in Oil and Gas Wells. Corrosion/89, Paper no. 466*. NACE International; 1989.
3. Ilman MN, Kusmono. Analysis of internal corrosion in subsea oil pipeline. *Case StudEng Fail Anal*. 2014;2(1):1-8. https://doi.org/10.1016/j.csefa.2013.12.003
4. Zhao G, Lu X, Xiang J, Han Y. Formation characteristic of CO_2 corrosion product layer of P110 steel investigated by SEM and electrochemical technique. *J Iron Steel Res Int*. 2009;16(4):89-94.
5. Lee K. *A Mechanistic Modeling of CO_2 Corrosion of Mild Steel in Presence of H2S*. [Ph.D thesis]. Ohio University; 2004.
6. Rodriguez M, Delgado D, Gonzalez R, et al. Corrosive wear failure analysis in a natural gas pipeline. *Wear*. 2007;263:567-571.
7. Nesic S. Key issues related to modelling of internal corrosion of oil and gas pipelines – a review. *Corros Sci*. 2007;49:4308-4338.
8. Bhandari J, Khan F, Abbassi R, Garaniya V, Ojeda R. Modelling of pitting corrosion in marine and offshore steel structures – a technical review. *J Loss Prevent Process Indust*. 2016;37:39-62.
9. Kamsu-Foguem B. Information structuring and risk-based inspection for the marine oil pipelines. *Appl Ocean Res*. 2016;56:132-142.
10. Kiefner JF, Vieth PH. New method corrects criterion for evaluating corroded pipe. *Oil Gas J*. 1990;6:56-59.
11. Ahammed M, Melchers RE. Reliability estimation of pressurized pipelines subject to localized corrosion defects. *Int J Press Vessels Piping*. 1996;69:267-272.
12. Ahammed M. Probabilistic estimation of remaining life of a pipeline in the presence of active corrosion defects. *Int J Press Vessels Piping*. 1998;75:321-330.
13. Melchers RE, Jeffrey RJ. Probabilistic models for steel corrosion loss and pitting of marine infrastructure. *Reliab Eng Syst Safety*. 2007;93(3):423-432.
14. Li S, Yu S, Zeng H, et al. Predicting corrosion remaining life of underground pipelines with a mechanically-based probabilistic model. *J Petrol Sci Eng*. 2009;65:162-166.
15. Netto T. A simple procedure for the prediction of the collapse pressure of pipelines with narrow and long corrosion defects - correlation with new experimental data. *Appl Ocean Res*. 2010;32(1):132-134.
16. Bazan F, Beck A. Stochastic process corrosion growth models for pipeline reliability. *Corros Sci*. 2013;74:50-58.
17. Larin O, Barkanov E, Vodka O. Prediction of reliability of the corroded pipeline considering the randomness of corrosion damage and its stochastic growth. *Eng Fail Anal*. 2016;66:60-71.

18. Leira BJ, Næss A, Næss OB. Reliability analysis of corroding pipelines by enhanced Monte Carlo simulation. *Int J Press Vessels Piping*. 2016; 144:11-17.
19. ASME-B31G. Manual for determining the remaining strength of corroded pipelines. *A Supplement of ASME B31G Code for Pressure Piping*. American Society for Mechanical Engineers; 1995.
20. de Waard C, Milliams DE. Prediction of Carbonic Acid Corrosion in Natural Gas Pipelines, in: First International Conference on the Internal and External Corrosion of Pipes, paper F1, University of Durham; 1975
21. de Waard C, Lotz U. *Prediction of CO_2 Corrosion of Carbon Steel, Corrosion/93, Paper*. Vol no. 69. NACE International; 1993.
22. Dugstad A, Lunde L, Videm K. *Parametric Study of CO_2 Corrosion of Carbon Steel, Corrosion/94, Paper*. Vol no. 14. NACE International; 1994.
23. NORSOK M-506 CO_2 corrosion Rate Model. (2005). https://www.standard.no/en/sectors/energi-og-klima/petroleum/norsok-standard-categories/m-material/m-5061/. Accessed July 23, 2020.
24. Nesic S, Nordsveen M, Maxwell N, Vrhovac M. Probabilistic modelling of CO_2 corrosion laboratory data using neural networks. *Corros Sci*. 2001;43:1373-1392.
25. Yao Y, Yang Y, Wang Y, Zhao X. Artificial intelligence-based hull structural plate corrosion damage detection and recognition using convolutional neural network. *Appl Ocean Res*. 2019;90:101823.
26. Sanchez JF, Alhama F, Moreno JA. An efficient and reliable model based on network method to simulate CO_2 corrosion with protective iron carbonate films. *Comput Chem Eng*. 2012;39:57-64.
27. Khakzad N, Khan F, Amyotte F. Safety analysis in process facilities: comparison of fault tree and Bayesian network approaches. *Reliab Eng Syst Safety*. 2011;96:925-932.
28. Shabarchin O, Tesfamariam S. Internal corrosion hazard assessment of oil & gas pipelines using Bayesian belief network model. *J Loss Preven Process Indus*. 2016;40:479-495.
29. Ayello F, Liu G, Zhang J. Decision making through the application of Bayesian network for internal corrosion assessment of pipelines. Proceedings of the ASME 2018 37th International Conference on Ocean, Offshore and Arctic Engineering. Volume 4: Materials Technology. Madrid, Spain. June 17–22; 2018.
30. Arzaghi E, Abbassi R, Garaniya V, et al. Developing a dynamic model for pitting and corrosion-fatigue damage of subsea pipelines. *Ocean Eng*. 2018;150:391-396.
31. Abubakirov R, Yang M, Khakzad N. A risk-based approach to determination of optimal inspection intervals for buried oil pipelines. *Process Safety Environ Protect*. 2020;134:95-107.
32. Yazdi M, Khan F, Abbassi R. Operational subsea pipeline assessment affected by multiple defects of microbiologically influenced corrosion. *Process Safety Environ Protect*. 2022;158:159-171.
33. Cai B, Shao X, Liu Y, et al. Remaining useful life estimation of structure systems under the influence of multiple causes: subsea pipelines as a case study. *IEEE Trans Indus Electron*. 2020;67(7):5737-5747.
34. Cai B, Sheng C, Gao C, et al. Artificial intelligence enhanced reliability assessment methodology with small samples. *IEEE Trans Neural Netw Learn Syst*. 2021;1-13. doi:10.1109/TNNLS.2021.3128514
35. Khakzad N, Van Gelder P. Vulnerability of industrial plants to flood-induced natechs: A Bayesian network approach. *Reliab Eng Syst Safety*. 2018;169:403-411.
36. Peng S, Zeng Z. An experimental study on the internal corrosion of a subsea multiphase pipeline. *Petroleum*. 2015;1(1):75-81.
37. Pearl J. *Probabilistic Reasoning in Intelligent Systems*. Morgan Kaufmann; 1988.
38. Neapolitan R. *Learning Bayesian Networks*. Prentice Hall; 2003.
39. Ricker RE. Analysis of pipeline steel corrosion data from NBS (NIST) studies conducted between 1922-1940 and relevance to pipeline management. *J Res Natl Instit Stand Technol*. 2010;115(5):373-392.
40. NORSOK Standard M-506. Draft 1 for Rev. 2, March. 2005. https://wiki.olisystems.com/wiki/images/e/eb/Norsok_standard_M-506.pdf. Accessed December 12, 2021.
41. GeNIe. Academic Installer, Decision Systems Laboratory, University of Pittsburg. https://download.bayesfusion.com/files.html?category=Academia. Accessed July 10, 2021.
42. DNV. Corroded Pipelines Recommended Practice DNV-RP-F101, October 2010.
43. Opeyemi D, Patelli E, Beer M, Timashev S. *Comparative Studies on Assessment of Corrosion Rates in Pipelines as Semi-Probabilistic and Fully Stochastic Values*. International Conference on Applications of Statistics and Probability in Civil Engineering; 2015.
44. Hasan S, Khan F, Kenny S. Probability assessment of burst limit state due to internal corrosion. *Int J Press Vessels Piping*. 2012;89: 48-58.
45. Caleyo F, Velázquez J, Valor A, Hallen J. Probability distribution of pitting corrosion depth and rate in underground pipelines: a Monte Carlo study. *Corros Sci*. 2009;51:1925-1934.
46. Velazquez JC, Caleyo F, Valor A, Hallen JM. Predictive model for pitting corrosion in buried oil and gas pipelines. *Corrosion*. 2009;65: 332-342.
47. Bubenik T, Olson R, Stephens D & Francini R Analyzing the pressure strength of corroded pipeline. In Proc. 11th Int. Conference on Offshore Mechanics and Arctic Engineering. Vol V, Part A, ASME 1992, pp.225–231.
48. Baker M. *Stress Corrosion Cracking Studies, Integrity Management Program DTRS56-02-D-70036*. Department of Transportation; 2004.
49. Nahal M, Khelif R. Failure probability assessment for pipeline under the corrosion effect. *Am J Mech Eng*. 2014;2(1):15-20.
50. Cabrini M, Lorenzi S, Pastore T. Corrosion behavior of carbon steels in CCTS environment. *Int J Corros*. 2016;3121247. doi:10.1155/2016/3121247

How to cite this article: Khakzad S, Yang M, Lohi A, Khakzad N. Probabilistic failure assessment of oil pipelines due to internal corrosion. *Process Saf Prog*. 2022;1-11. doi:10.1002/prs.12364

APPENDIX A: Application of maximum likelihood function

Consider a BN consisting of three binary nodes, two root nodes X and Y, and a child node Z. X, Y, and Z as discrete random variables can assume values of 0 or 1. Given a dataset as in Table 4, the probability of ($z = 1 \mid x = 1, y = 0$), among others, can be estimated using the MLE algorithm. To do so, the estimated probabilities can be presented as $\theta = \widehat{P}(z = 1 \mid x = 1, y = 0)$ and $1 - \theta = \widehat{P}(z = 0 \mid x = 1, y = 0)$.

As such, the likelihood function (L) for observing the data pairs listed on lines 2, 4, 9, and 10 in Table 4 can be developed as

$$L = \theta \times (1 - \theta) \times \theta \times \theta = \theta^3 - \theta^4$$

To find the value of θ that maximizes the likelihood function, we can calculate the first derivative of the likelihood function with respect to θ, and then solve for the value of θ that makes this derivative equal to zero:

TABLE 4 Exemplary dataset to estimate the conditional probability of Z given X and Y

Line No.	X	Y	Z
1	1	1	1
2	1	0	1
3	0	0	0
4	1	0	0
5	0	1	1
6	0	0	1
7	0	0	0
8	1	1	0
9	1	0	1
10	1	0	1
11	1	1	1
12	0	1	0

$$\frac{\partial L}{\partial \theta} = 3\theta^2 - 4\theta^3 = 0 \rightarrow \theta^2(3-4\theta) = 0 \rightarrow \theta = \frac{3}{4}$$

Therefore, $\widehat{P}(z=1|x=1,y=0) = \frac{3}{4}$.

As explained in Section 2.2, one may decide to maximize the log-likelihood function to find the value of θ:

$$\text{Log}\, L = \text{Ln}\left(\theta^3 \times (1-\theta)\right) = 3\text{Ln}(\theta) + \text{Ln}(1-\theta)$$

$$\frac{\partial(\text{Log}\, L)}{\partial \theta} = \frac{3}{\theta} - \frac{1}{1-\theta} = 0 \rightarrow \theta = \frac{3}{4}$$

Using the MLE algorithm, the CPTs of nodes pH, Shear, and Corrosion rate in the BN have been determined by GeNIe.[41] The CPT of node pH is shown in Table 5 as an example.

TABLE 5 CPT of node pH in the BN in Figure 3, which has been developed using the MLE algorithm in GeNIe[41]

				pH		
No.	pCO_2	T	P	pH1	pH2	pH3
1	*C*1	*T*1	*P*1	0.033	0.033	0.933
2	*C*1	*T*1	*P*2	0.033	0.033	0.933
3	*C*1	*T*1	*P*3	0.033	0.033	0.933
4	*C*1	*T*2	*P*1	0.033	0.033	0.933
5	*C*1	*T*2	*P*2	0.033	0.033	0.933
6	*C*1	*T*2	*P*3	0.033	0.033	0.933
7	*C*1	*T*3	*P*1	0.033	0.033	0.933
8	*C*1	*T*3	*P*2	0.033	0.033	0.933
9	*C*1	*T*3	*P*3	0.033	0.033	0.933
10	*C*2	*T*1	*P*1	0.033	0.933	0.033
11	*C*2	*T*1	*P*2	0.033	0.933	0.033
12	*C*2	*T*1	*P*3	0.033	0.933	0.033
13	*C*2	*T*2	*P*1	0.033	0.933	0.033
14	*C*2	*T*2	*P*2	0.033	0.933	0.033
15	*C*2	*T*2	*P*3	0.033	0.933	0.033
16	*C*2	*T*3	*P*1	0.033	0.933	0.033
17	*C*2	*T*3	*P*2	0.033	0.933	0.033
18	*C*2	*T*3	*P*3	0.033	0.933	0.033
19	C3	*T*1	*P*1	0.933	0.033	0.033
20	*C*3	*T*1	*P*2	0.933	0.033	0.033
21	*C*3	*T*1	*P*3	0.933	0.033	0.033
22	*C*3	*T*2	*P*1	0.933	0.033	0.033
23	*C*3	*T*2	*P*2	0.033	0.933	0.033
24	*C*3	*T*2	*P*3	0.033	0.933	0.033
25	*C*3	*T*3	*P*1	0.033	0.933	0.033
26	*C*3	*T*3	*P*2	0.033	0.933	0.033
27	*C*3	*T*3	*P*3	0.033	0.933	0.033